

# Multipacting in 1.5-GHz superconducting niobium cavities of the CEBAF shape\*

J. Knobloch, W. Hartung, and H. Padamsee  
 Floyd R. Newman Laboratory of Nuclear Studies  
 Cornell University, Ithaca, New York 14853

## Abstract

We present definitive thermometric evidence of two-point multipacting in the CEBAF cavity shape, starting at  $E_{pk} = 30$  MV/m (at 1.5 GHz). With the aid of high speed thermometry, we were able to record fleeting multipacting events near the cavity equator. Short term electron bombardment eliminates the multipacting barrier. Numerical trajectory simulations presented here also confirm the experimental data. Although multipacting itself could be processed away and did not limit the cavity performance, it is shown that the quenches due to the electron bombardment increase the cavity's residual resistance by creating and trapping magnetic flux.

## 1 Introduction

Multipacting in radio-frequency (rf) cavities<sup>1</sup> is a resonant process, in which a large number of electrons build up an avalanche, absorbing rf power so that it becomes impossible to increase the cavity fields by raising the incident power. [1] The electrons collide with cavity's walls, leading to a large temperature rise and eventually to thermal breakdown (in the case of superconducting cavities).

Before the invention of spherically (and elliptically) shaped cavities, the onset of multipacting was usually recognized when the field level in the cavity remained fixed, as if a barrier were present, even as more rf power was supplied. In effect, the quality  $Q$  of the cavity abruptly reduced at the multipacting threshold.

In many cases, it is found that such a multipacting barrier can be surmounted by "processing." This is done by allowing multipacting to progress for several minutes, while slowly raising the rf power. Eventually, and sometimes abruptly, the  $Q$  improves and the multipacting ceases. In general, once multipacting barriers have been processed, they do not reappear, provided the cavity is kept under vacuum. However a barrier may reappear after the cavity is exposed to air, which indicates that multipacting is strongly dependent on the condition of the first few monolayers of the rf surface. Surface adsorbates can also strongly affect the multipacting behavior.

One-point multipacting [1] was common in cavities of older design, such as the muffin-tin cavity. This problem was eliminated with the invention of the spherical/elliptical cavity shape. [2] However, there were indications that two-point multipacting [1] still occurred on rare occasions. First observations of such occurrences along the cavity equator were made at CERN with LEP cavities. [3] Figure 1 depicts a temperature map of multipacting in progress. In this case, multipacting could only be eliminated after several hours of processing. However, this type of multipacting could be avoided altogether with special care in cleanliness and drying.

Two-point multipacting in elliptical cavities of the CEBAF shape has not been directly observed in the past, although indirect evidence of such activity has been reported by KEK, starting at a peak electric field of about  $E_{pk} = 30$  MV/m (at 1.5 GHz). [4] However, the use of high speed thermometry [5, 6] has now permitted us to observe directly the heating due to very short lived multipacting in single-cell elliptical (LE1) cavities of the CEBAF shape along the equator, again starting at 30 MV/m. Three types of LE1 cavities (Mark I, Mark II, and Mark III), with only minor shape differences, were tested. Only Mark I cavities showed repetitive multipacting, although the other two shapes were involved in singular multipacting events. This fact, together with other evidence to be presented, indicates that the secondary electron emission coefficient (SEC) for the impacting multipacting electrons is very close to unity.

---

\*Supported by the National Science Foundation with supplementary support under the US-Japan Agreement.

<sup>1</sup>as well as in other rf structures

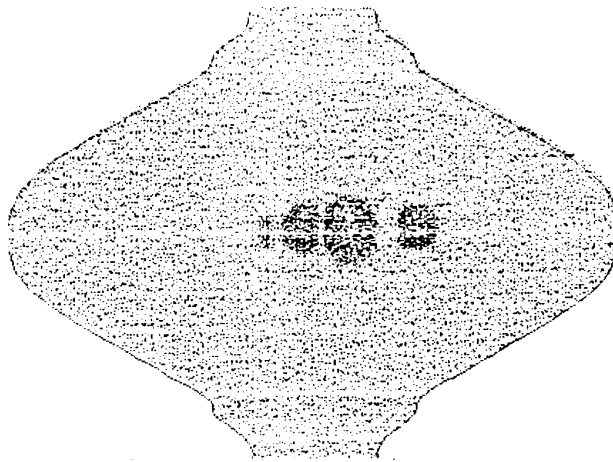


Figure 1: Temperature map of a 350 GHz LEP cavity. Dark regions denote high temperatures. The hotspots on opposite sides of the equator reveal two-point multipacting in progress. The peak temperature rise ( $\Delta T$ ) was about 1.4 K. [3]

Numerical simulations of multipacting trajectories with the computer code MULTIP confirm the presence of stable multipacting trajectories in Mark I cavities, but not in Mark II and Mark III cavities. In all three cases the SEC was taken to exceed unity above 20 eV. The predicted multipacting threshold field also agrees well with the experimental evidence.

On account of the fact that the SEC is very close to unity, the multipacting barriers can easily be surmounted by processing for as little as 20 seconds. However, the quenches that result from the multipacting heating create magnetic flux via thermal gradients, by the same mechanism reported on in References [6, 7]. As the cavity reverts back to the superconducting state, this flux can be trapped, resulting in an increased residual resistance in the multipacting region.

## 2 Experimental setup

The experimental setup to study L-band cavities has been described in a number of papers [5, 6, 8] and will not be repeated here in detail. The main diagnostic tool is a fixed-array thermometry system comprising 756 thermometers attached to the cavity exterior, capable of mapping the cavity temperature distribution in superfluid helium at 1.6 K. Important to the study of multipacting are the system's short acquisition times for a temperature map ( $\approx 0.14$  s), and its high resolution (as good as  $30 \mu\text{K}$ ). An automated  $Q$  versus  $E_{\text{pk}}$  measurement system operates in conjunction with the thermometry system, to provide information on the integrated cavity losses.

Single-cell cavities were made with  $\text{RRR} = 250$  niobium using available dies for multicell cavities. Three different shapes, termed Mark II (center cell), Mark III (end cell) and Mark I (early design no longer employed for multicell cavities), were used. Nominally, the shapes of all our LE1 cavities are the same. However, there are subtle differences (on the order of millimeters). The shape parameters are given in the Appendix.

The cavity preparation prior to testing consisted of the standard chemical treatment [6, 9] (one hour in nitric acid to remove any remaining indium and about five minutes in buffered chemical polish (BCP 1:1:2)). A rinse with deionized water for one hour followed the chemical etch, before drying the cavity with hot, filtered nitrogen gas and mounting the cavity on the test stand.

## 3 Multipacting in Mark I cavities

### 3.1 Breakdown events

During a typical test of a Mark I cavity (LE1-21), the fields would periodically collapse once every few seconds when a threshold field of  $E_{\text{pk}} \approx 30$  MV/m was exceeded. For reasons that will soon become apparent, we conclude that these events were due to multipacting. The self-pulsing continued for about 20 seconds, after which the fields in the cavity could be raised further, before a similar phenomenon was again encountered at

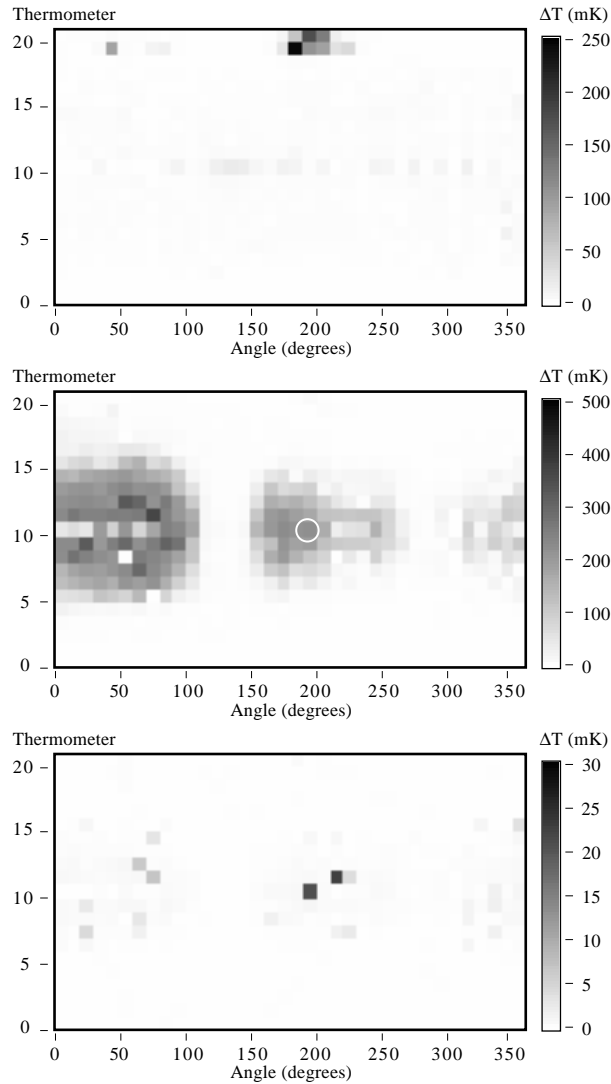


Figure 2: Series of temperature maps taken during a test of cavity LE1-21 (Mark I shape) while multipacting was active at  $E_{pk} \approx 34$  MV/m. The map interval is about 0.15 s. Thermometers 1 and 19 are located on the bottom and top iris of the cavity, respectively, and thermometer 10 is located at the cavity equator.

a slightly higher field level. By processing through these weak multipacting barriers, we eventually were able to achieve  $E_{pk} = 38$  MV/m. At that point field emission and related thermal breakdown prevented us from reaching higher fields.

Figure 2 depicts three temperature maps taken in rapid succession (0.15 s intervals) to capture transient events. The first map depicts the temperature distribution at  $E_{pk} \approx 30$  MV/m, just before a breakdown event. A field emitter is visible at the top iris at  $190^\circ$ . The breakdown event is recorded in the following map. Significant heating is visible over a large fraction of the cavity, the high temperature region being centered on the equator. Within less than 0.15 s the fields have completely collapsed and the cavity cools (third map). The temperature of the circled thermometer as a function of time is displayed in Figure 3 to illustrate the repetitive nature of the breakdown.

We found that the breakdown events commence when the temperature, or equivalently  $E_{pk}$ , exceeds a threshold value. Although this behavior has some similar features to defect induced thermal breakdown, the four observations below show that a defect cannot be the cause of the quenches.

1. The temperatures recorded during breakdown never exceeded a few hundred millikelvin. Defect related thermal breakdown, on the other hand, usually results in temperature rises at the defect far exceeding 1000 mK.

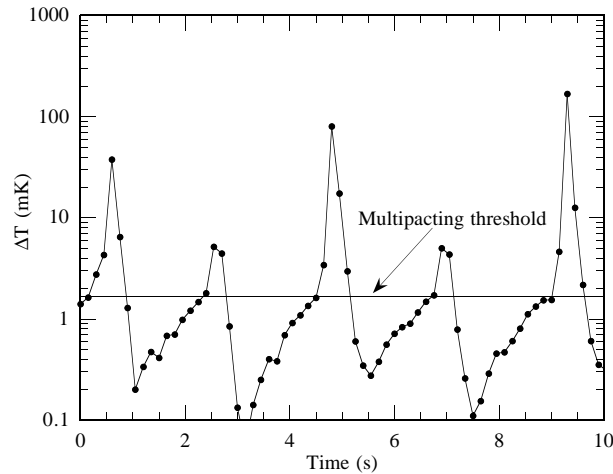


Figure 3: Temporal evolution of the temperature recorded by the thermometer circled in Figure 2. Note the logarithmic temperature scale.

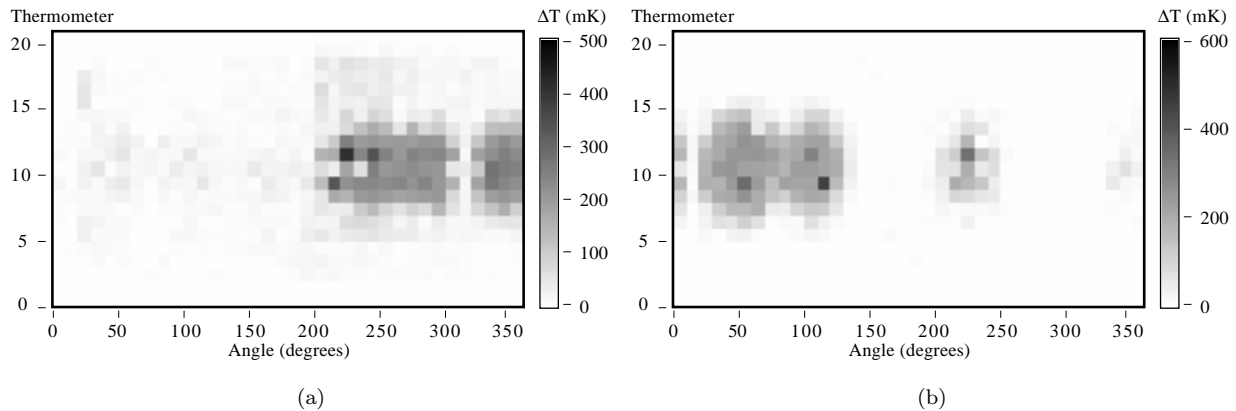


Figure 4: Multipacting related breakdown at two different times in cavity LE1-17 (Mark I shape). The peak electric field was about 32 MV/m.

2. Several distinct areas in the equator region of the cavity show breakdown related heating rather than being centered on a singular defect.
3. Defect related thermal breakdown cannot be processed away, whereas we had no trouble increasing  $E_{pk}$  after 20 s or so of processing.
4. Subsequent breakdown events originate in different parts of the cavity, as shown in Figure 4.

Once the cavity had been “conditioned” at a given field level, no further breakdown events were recorded up to that field. However, upon thermally cycling to room temperature, reconditioning of the cavity was required as breakdown was again encountered, starting at about 30 MV/m. As we will discuss, this is a characteristic feature of multipacting.

### 3.2 Low field losses

Breakdown events occurred only at field levels of 30 MV/m and higher. Yet, similar to events recorded during thermal breakdown [6, 7], the low field resistance of the cavity was affected by the multipacting. Figure 5 depicts the ratio of the cavity’s low field surface resistance ( $R_s$ ) after and before a series of breakdown events. Most of the equator region increased its  $R_s$  dramatically, although some areas actually reduced their losses. The remainder of the cavity was largely unaffected. Overall, the region covered by the equator thermometers and their nearest neighbors increased its surface resistance by more than a factor of two. Thermometers further from the equator registered little change. Individual sites increased their surface resistance more (see Figure 6(a)).

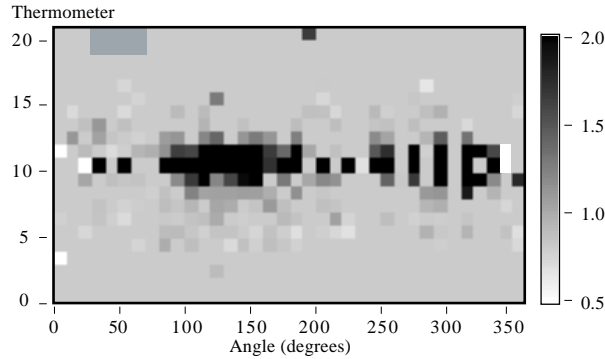


Figure 5: Ratio of the surface resistance after and before a series of breakdown events in cavity LE1-21. Dark regions represent increased surface resistance, while light regions show decreases in resistance.

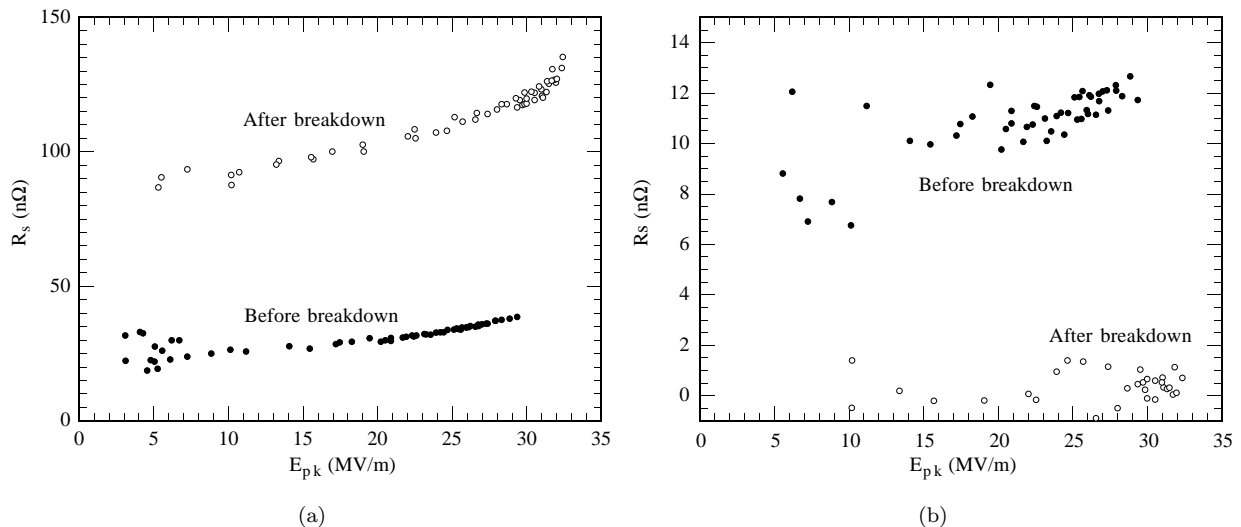


Figure 6: Surface resistance versus  $E_{pk}$  before and after breakdown. (a) Equator site at  $140^\circ$  which increased  $R_s$  during breakdown, and (b) equator site at  $340^\circ$  which reduced  $R_s$  during breakdown.

Increases by as much as a factor of seven were recorded. Also, a few sites reduced their  $R_s$  close to zero (see Figure 6(b)).

A given site could change its surface resistance numerous times following repeated breakdown events. In some cases, the surface resistance would increase several times (Figure 7(a)), so that in the end a total increase by as much as a factor of 6-10 was recorded. Other sites initially increased their surface resistance, only to reduce  $R_s$  to intermediate levels during a subsequent breakdown event (Figure 7(b)).

Following thermal cycling to room temperature, all  $R_s$  changes due to breakdown were reversed and the original  $R_s$  “landscape” was recovered. Thermal cycles to intermediate temperatures  $T_c < T < T_{room}$  were not attempted with this cavity. However, other cavities (to be discussed later) underwent breakdown events similar to those described here. In these cases, increases and reductions of  $R_s$  along the equator were also observed but only regions that increased  $R_s$  recovered their original values following a cycle to intermediate temperatures. [6]

## 4 Discussion

The  $R_s$  changes described here are reminiscent of the low field losses resulting from defect induced thermal breakdown. [6, 7] Again, we suspect that the increased losses are due to flux generation by thermocurrents during the breakdown events and its subsequent trapping as the cavity is rapidly cooled through  $T_c$ . This effect is discussed in detail in References [6, 7].

However, here no single defect can be responsible for initiating the quenches discussed above. Since the low

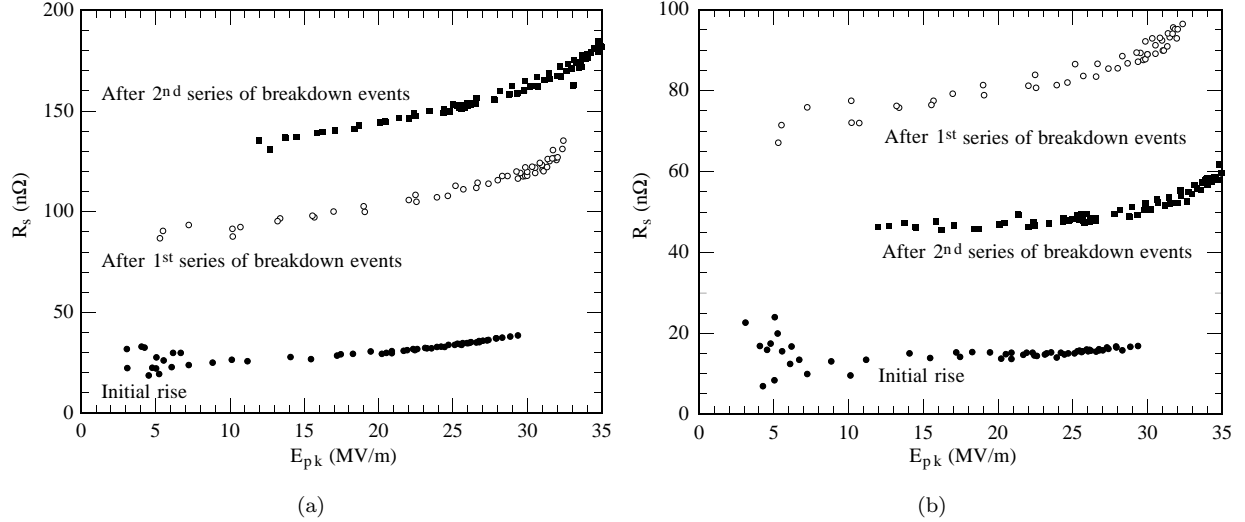


Figure 7: Effect of multiple breakdown events on the surface resistance of individual sites in cavity LE1-21. (a) Equator site at  $140^\circ$  and (b) equator site at  $150^\circ$ .

field losses are only affected by the breakdown mechanism in a thin band centered on the equator, the results suggest that the breakdown *source* is concentrated along the equator, creating large thermal gradients in this narrow region.

These observations are consistent with multipacting as the cause of the breakdown. According to simulations (discussed below) the threshold field for multipacting should be 30 MV/m, which is the level at which breakdown was first observed experimentally as well. Only sites on or close to the cavity equator change their  $R_s$  during breakdown, indicating that this region must be involved in electron bombardment concentrated about the equator that ultimately results in a quench and flux trapping. Judging from the symmetrical heating about the equator, multipacting is likely to be of a two-point nature. Due to the strong magnetic field in this area, the normal conducting region grows rapidly to cover a large portion of the cavity, as confirmed by the temperature maps. Since we were readily able to process through the breakdown, the multipacting electron energies must lie close to the points where the secondary electron coefficient (SEC) of the rf surface crosses one (lower and upper crossover).

#### 4.1 Multipacting simulations

To confirm our hypothesis, we ran multipacting simulations similar to those described in Reference [1]. We used the finite element code SUPERLANS [10, 11] to solve for the electromagnetic fields of the cavity ( $TM_{010}$ ) mode at one value of  $E_{pk}$ . The program MULTIP [12, 13] then used the field distribution to calculate trajectories for electrons emitted at numerous points  $S_0^{(j)}$  of the cavity wall and at various emission phases  $\varphi_0^{(j)}$ . The electric field was also varied.

For each pair  $(S_0^{(j)}, \varphi_0^{(j)})$  the electron trajectory was integrated until it impacted a cavity wall. When this happened, a new electron was emitted at that site, provided the SEC at the impact energy exceeded one *and* the electric field pointed towards the wall. If one (or both) of these conditions was not satisfied, then the number of electron generations created up until this point was recorded, and calculations were started for a new pair  $(S_0^{(j)}, \varphi_0^{(j)})$  and/or another value for  $E_{pk}$ . Trajectory calculations for a given  $(S_0^{(j)}, \varphi_0^{(j)})$  pair were terminated when the 40<sup>th</sup> generation was created, the assumption being that a stable multipacting trajectory had been found.

Electron emission energies used in the calculations ranged from 0 eV to 3 eV, and  $E_{pk}$  was varied from 0 to 50 MV/m. The SEC was taken to be greater than one between 20 eV and 3000 eV. These values are reasonable for a wet treated niobium surface. [14]

Depicted in Figure 8 is the highest electron generation recorded for all simulated  $(S_0^{(j)}, \varphi_0^{(j)})$  pairs as a function of  $E_{pk}$ . We see that Mark I cavities are predicted to be multipacting free only up to about 32 MV/m, a value that is very close to our experimental observations of breakdown.

Our calculations showed that electron trajectories starting a fair distance from the equator drift towards the equator within a few generations. It is for this reason that elliptical cavities are so effective at suppressing

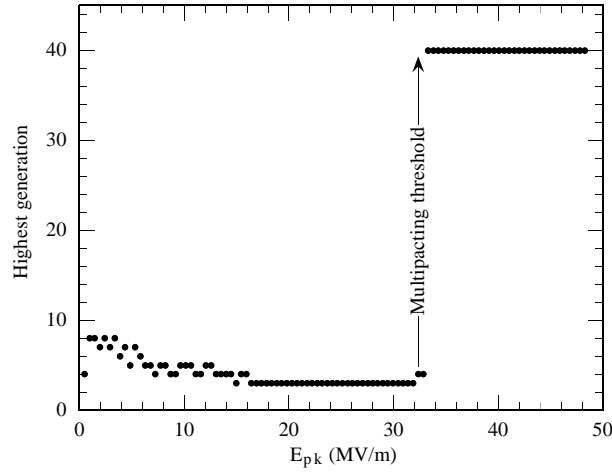


Figure 8: Highest electron generation recorded for all simulated  $(S_0^{(j)}, \varphi_0^{(j)})$  pairs versus  $E_{pk}$  for Mark I cavities. A trajectory calculation was automatically stopped when the 40<sup>th</sup> generation was reached, the assumption being that a multipacting trajectory had been found. The electron emission energy was 3 eV.

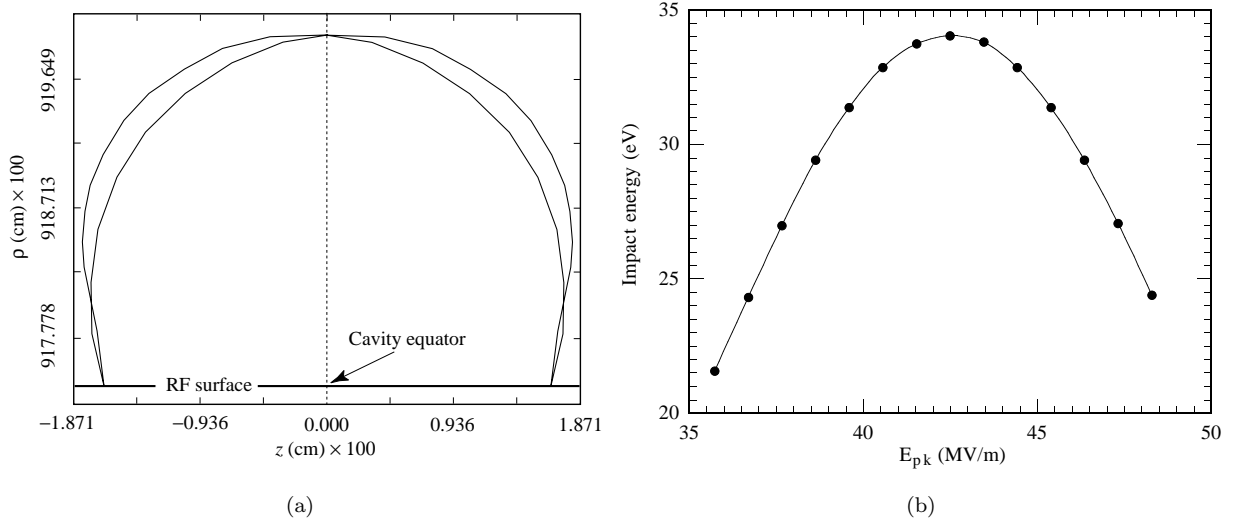


Figure 9: (a) Stable, two-point multipacting trajectories at 37 MV/m near the equator of Mark I cavities. Secondary emission was perpendicular to the rf surface. (b) Electron impact energy as a function of  $E_{pk}$ .

one-point multipacting. [2] However, for  $E_{pk} \geq 32$  MV/m electrons emanating within only 0.2 mm of the equator (with an initial energy of 2 or 3 eV) follow a trajectory to the symmetry point on the other side of the equator in  $1/2$  an rf period. Secondaries released at the impact site then follow a similar path back to the originator location. An example of the trajectories is shown Figure 9(a). This situation constitutes two-point multipacting of the first order. Two narrow ranges of start phases, separated by  $1/2$  an rf cycle, lead to this type of multipacting. ( $2\pi \times 0.32 < \varphi_0 < 2\pi \times 0.38$  and  $2\pi \times 0.82 < \varphi_0 < 2\pi \times 0.88$ .)

Depicted in Figure 9(b) are the electron impact energies as a function of  $E_{pk}$  if the secondaries are emitted with an energy of 2 eV. As predicted by experiment, the energies are very close to the lower crossover of the SEC.<sup>2</sup>

Our simulations indeed confirm the hypothesis that the electron impact energies are very close to the lower crossover. Desorption of surface adsorbates by electron bombardment and possibly even a local gas discharge will lower the SEC, thereby arresting multipacting. The regions that reduce  $R_s$  during the multipacting process are indicative of the desorption process. Desorption also explains why the multipacting center constantly shifts

<sup>2</sup>When the emission energy was increased to 3 eV, or the emission direction was tilted by  $30^\circ$ , the impact energies increased slightly, so that the curve in Figure 9(b) shifted to lower  $E_{pk}$  values. In these cases the impact energy exceeded 20 eV slightly below 32 MV/m.

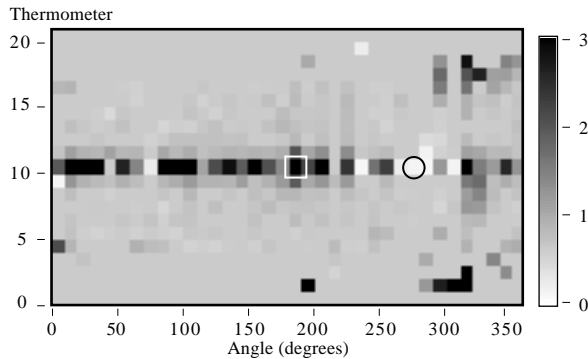


Figure 10: Surface resistance ratio map of cavity LE1-20 at 11.3 MV/m after and before a breakdown event was observed at  $E_{pk} = 30$  MV/m. The increases recorded near the iris around  $310^\circ$  are field emission related and not due to the breakdown event.

to different places of higher SEC around the equator (Figure 4). The resultant change in surface composition then arrests the multipacting. Our interpretation is supported by the fact that thermal cycling reactivates multipacting at the lowest field ( $\approx 30$  MV/m) presumably by redistributing gases in the cavity. We know that such a redistribution of gases does take place, because the regions which *reduced* their losses during multipacting reverted back to their original  $R_s$  after a complete room temperature cycle, whereas they were unaffected by intermediate thermal cycles.

Note that the impact energy rises with increasing field up to at least the low 40 MV/m's. It therefore is not surprising that multipacting reappeared at successively higher fields when we raised the fields for the first time. At each field level, multipacting progressed until the SEC was lowered below one. Then, when the field was increased again, the impact energy rose and the SEC exceeded unity once more. Further processing was then required before higher fields could be attained. Provided the cleanliness of the rf surface is maintained, and it is not re-exposed to gases, multipacting is no longer active at lower fields. In cavity LE1-21 multipacting continued up to the maximum field attained (38 MV/m). Based on Figure 9(b) we expect that multipacting would have been active up to about 42.5 MV/m if the cavity had not been limited by thermal breakdown.

## 5 Multipacting in Mark II and Mark III cavities

Our trajectory simulations did not predict sustained multipacting in Mark II and Mark III cavities. Correspondingly we did not observe repetitive multipacting induced breakdown (as in cavities LE1-17 and LE1-21) in any of the five Mark II and Mark III cavities we tested that exceeded 30 MV/m. These results show that even very subtle alterations to the cavity shape can have a significant impact on multipacting.

However, in all but one Mark II/III cavity which reached  $E_{pk} = 30$  MV/m we did observe singular breakdown events that affected the low field properties of the cavity. [6] All of these isolated breakdown events occurred at fields close to 30 MV/m. They are suggestive of short lived multipacting activity.

In many cases the single breakdown event resulted in increased low field losses along the cavity equator similar to that in Figure 5. Again, some sites reduced their  $R_s$  during these events. Figure 10, for example, illustrates the changes of  $R_s$  observed in cavity LE1-20, which broke down at 30 MV/m.<sup>3</sup> The region around  $270^\circ$  showed a marked resistance reduction due to the breakdown event, whereas most of the remainder of the equator increased its surface resistance. The test was followed by a thermal cycle to about 12 K, which removed the increased losses along the equator (Figure 11(a)). However, the region around  $270^\circ$  remained unaffected (see Figure 11(b)). A complete thermal cycle to room temperature was required to restore the original  $R_s$ .

The fact that only a room temperature cycle restores the surface resistance emphasizes that the mechanism resulting in increased losses is not identical with that responsible for the reduction of  $R_s$  in other regions. Increased losses disappear when the cavity temperature is raised to 12 K, demonstrating that these losses are due to breakdown induced flux trapping (as discussed in References [6, 7].)

Since a temperature cycle to 300 K is required to restore the  $R_s$  in low loss regions, we suspect that the reduction of losses results from the desorption of gases. The desorption process can be from the bombardment of

<sup>3</sup>A field emitter had limited the cavity to 20 MV/m, at which point it rf processed. Due to the reduced power dissipation in the cavity, the field rose rapidly to 30 MV/m, and some short-lived self pulsing of the cavity was observed.

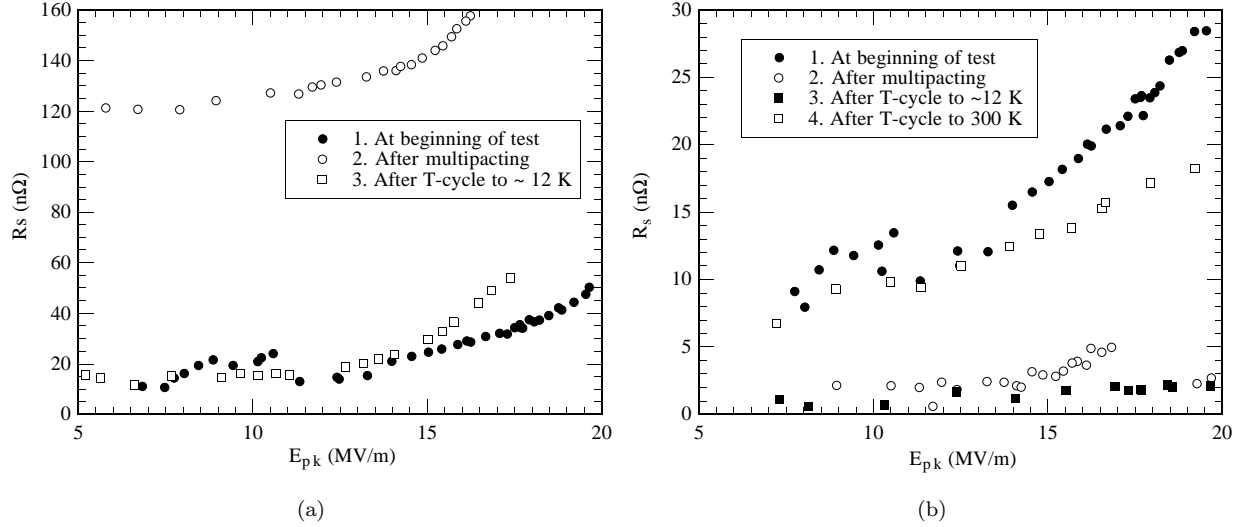


Figure 11: (a) Surface resistance at the framed site in Figure 10 as a function of  $E_{pk}$ . A thermal cycle to  $\approx 12$  K was sufficient to remove the additional losses due to multipacting. (b) Plot of the surface resistance of the circled site. A complete thermal cycle was required to restore the  $R_s$  to its initial value.

the surface by multipacting electrons directly, or due to a gas discharge initiated by the multipacting current [15] and/or the electric field. Elevated temperatures associated with room temperature cycling are then required to redistribute the gases throughout the cavity and to restore the  $R_s$ .

All our observations with Mark II and Mark III cavities show that multipacting in these shapes is very short lived. [6] Only one or two breakdown events are observed in these cavities, and subsequent processing times are sufficient to suppress multipacting altogether. Unlike Mark I cavities, thermal cycling to room temperature does *not* restore multipacting in Mark II and Mark III cavities. The electron impact energies must therefore lie *very* near the lower crossover of the SEC. The slight differences in shape that do exist between Mark I and Mark II/III cavities must be responsible for shifting the impact energy slightly below 20 eV.

## 6 Summary

Two point multipacting at the equator has been observed in Mark I, LE1 cavities between  $E_{pk} = 30$  and 38 MV/m. Repetitive collapse of the cavity fields and associated short term enhanced heating along the equator are the signature of multipacting.

Trajectory calculations confirm that two point multipacting at the equator is possible above about 32 MV/m. The electron impact energy is very low so that multipacting processes after only a few breakdown events due to the desorption of adsorbates. However, the redistribution of gases following a thermal cycle to room temperature is sufficient to reactivate the multipacting.

Although the multipacting in LE1 cavities itself is quite benign and can readily be processed, it increases the low field losses by trapping magnetic flux along the equator, where the heating by electron bombardment dominates. This effect is similar to that of thermal breakdown. [6, 7]

Very fleeting multipacting activity was also observed in Mark II and Mark III cavities. Again, these events led to flux trapping. Trajectory calculations do not predict sustained multipacting when using a secondary emission coefficient that exceeds one between 20 eV and 3000 eV. The slight difference in cavity shape between Mark I and Mark II/III cavities must be responsible for the lowering of the impact energy to 20 eV or below.

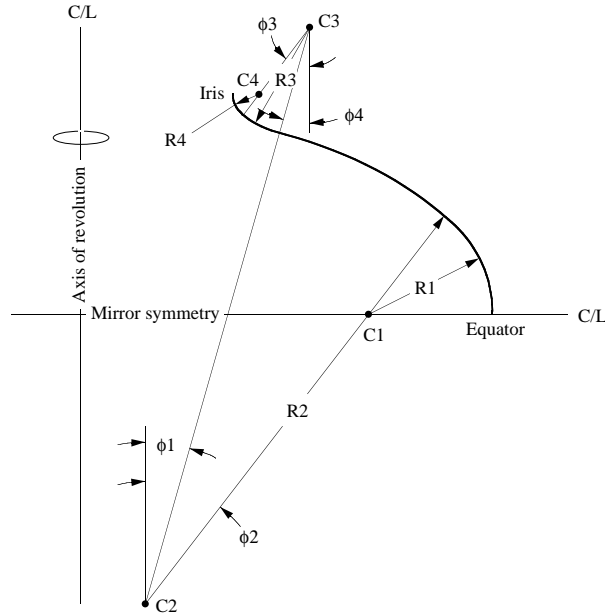


Figure 12: Contour of a quarter segment of the LE1 cavities used in rf tests. The parameters are given in Table 1.

Table 1: Parameters for the shape of Mark I, Mark II and Mark III LE1 cavities in Figure 12.

Parameter	Mark I	Mark II	Mark III
R1	2.963	2.828	2.892
C1X	6.239	6.575	6.422
C1Y	0.000	0.000	0.000
R2	10.108	11.122	10.646
C2X	1.812	1.516	1.658
C2Y	-5.610	-6.572	-6.118
R3	2.492	2.498	2.498
C3X	5.241	5.249	5.249
C3Y	6.515	6.526	6.526
R4	0.591	0.590	0.590
C4X	4.091	4.095	4.095
C4Y	5.001	5.006	5.006
$\phi_1$	15.75°	15.89°	15.89°
$\phi_2$	38.29°	37.58°	37.58°
$\phi_3$	37.24°	37.22°	37.22°
$\phi_4$	15.97°	15.97°	15.97°

## A Cavity shapes

Figure 12 depicts the shapes of Mark I, Mark II, and Mark III LE1 cavities. Table 1 provides the appropriate parameters for the figure.

## References

- [1] H. Padamsee, J. Knobloch, and T. Hays, *RF Superconductivity for Accelerators*, Wiley and Sons, New York, 1998, To be published.
- [2] U. Kelin and D. Proch, in *Proceedings of the Conference on Future Possibilities for Electron Accelerators*, volume N1-17, Charlottesville, 1979.

- [3] W. Weingarten, Electron loading, in *2<sup>nd</sup> Workshop on RF Superconductivity*, edited by H. Lengeler, pages 551–582, CERN, Geneva, Switzerland, 1984.
- [4] K. Saito et al., Water rinsing of the contaminated superconducting rf cavities, in *Proceedings of the 7<sup>th</sup> Workshop on RF Superconductivity*, edited by B. Bonin, pages 379–383, Gif-sur-Yvette, France, 1995, Proceedings also published as internal Saclay report CEA/Saclay 96 080/1.
- [5] J. Knobloch, H. Muller, and H. Padamsee, *Review of Scientific Instruments* **65**, 3521 (1994).
- [6] J. Knobloch, *Advanced Thermometry Studies of Superconducting RF Cavities*, PhD thesis, Cornell University, 1997, Laboratory of Nuclear Studies thesis CLNS 97-3.
- [7] J. Knobloch and H. Padamsee, Flux trapping in niobium cavities during breakdown events, in *Proceedings of the 8<sup>th</sup> Workshop on RF Superconductivity*, Padua, Italy, 1997.
- [8] J. Knobloch and H. Padamsee, *Particle Accelerators* **53**, 53 (1996), Also published in the Proceedings of the 7<sup>th</sup> Workshop on RF Superconductivity, Gif-sur-Yvette, France, pp. 95–103 (1995).
- [9] P. Kneisel, Surface preparation of niobium, in *Proceedings of the Workshop on RF Superconductivity*, edited by M. Kuntze, pages 27–40, Karlsruhe, 1980, Proceedings also published as internal Kernforschungszentrum Karlsruhe report KFK-3019.
- [10] D. G. Myakishev and V. P. Yakovlev, An interactive code SUPERLANS for the evaluation of rf cavities and accelerating structures, in *Proceedings of the 1991 IEEE Particle Accelerator Conference*, pages 3002–3004, San Francisco, CA, 1991.
- [11] D. G. Myakishev and V. P. Yakovlev, The new possibilities of SUPERLANS code for evaluation of axis-symmetric cavities, in *Proceedings of the 1995 Particle Accelerator Conference and International Conference on High Energy Accelerators*, pages 2348–2349, Dallas, TX, 1995.
- [12] R. Ferraro, Field emission studies: An owner’s manual (Part V), Technical report, Cornell University, Laboratory of Nuclear Studies, 1996, SRF/D report 960703-08, edited by W. Hartung.
- [13] Field emission studies: An owner’s manual, Technical report, Cornell University, Laboratory of Nuclear Studies, 1991, SRF/D report 910121-24, edited by W. Hartung.
- [14] H. Piel, Superconducting cavities, in *CERN Accelerator School: Superconductivity in Particle Accelerators*, edited by S. Turner, pages 149–196, Hamburg, Germany, 1988, CERN publication 89-04.
- [15] F. Llewellyn-Jones, *Ionization and Breakdown in Gases*, Wiley, New York, 1957.